



**HAL**  
open science

# Tau Protein Discrete Aggregates in Alzheimer's Disease: Neuritic Plaques and Tangles Detection and Segmentation using Computational Histopathology

K Maňoušková, V Abadie, M Ounissi, G Jimenez, L Stimmer, B Delatour, S  
Durrleman, Daniel Racocceanu

## ► To cite this version:

K Maňoušková, V Abadie, M Ounissi, G Jimenez, L Stimmer, et al.. Tau Protein Discrete Aggregates in Alzheimer's Disease: Neuritic Plaques and Tangles Detection and Segmentation using Computational Histopathology. SPIE Medical Imaging 2022, Feb 2022, San Diego, United States. hal-03522378v1

**HAL Id: hal-03522378**

**<https://hal.science/hal-03522378v1>**

Submitted on 12 Jan 2022 (v1), last revised 31 Jan 2022 (v2)

**HAL** is a multi-disciplinary open access archive for the deposit and dissemination of scientific research documents, whether they are published or not. The documents may come from teaching and research institutions in France or abroad, or from public or private research centers.

L'archive ouverte pluridisciplinaire **HAL**, est destinée au dépôt et à la diffusion de documents scientifiques de niveau recherche, publiés ou non, émanant des établissements d'enseignement et de recherche français ou étrangers, des laboratoires publics ou privés.

# Tau Protein Discrete Aggregates in Alzheimer’s Disease: Neuritic Plaques and Tangles Detection and Segmentation using Computational Histopathology

K. Maňoušková, V. Abadie, M. Ounissi, G. Jimenez,  
L. Stimmer, B. Delatour, S. Durrleman, D. Racoceanu

Sorbonne Université, Institut du Cerveau - Paris Brain Institute - ICM, Inserm, CNRS,  
APHP, Hopital de la Pitié Salpêtrière, Paris, Fr

## ABSTRACT

Tau proteins in the gray matter are widely known to be a part of Alzheimer’s disease symptoms. They can aggregate in three different structures within the brain: neurites, tangles, and neuritic plaques. The morphology and spatial disposition of these three aggregates are hypothesised to be correlated to the advancement of the disease. In order to establish a behavioural disease model related to the Tau proteins aggregates, it is necessary to develop algorithms to detect and segment them automatically. We present a 4-folded pipeline aiming to perform with clinically operational results. This pipeline is composed of a non-linear colour normalisation, a CNN-based image classifier, an Unet-based image segmentation stage, and a morphological analysis of the segmented objects. The tangle detection and segmentation algorithms improve state-of-the-art performances (75.8% and 91.1% F1-score, respectively), as well as for neuritic plaques detection and segmentation (81.3% and 78.2% F1-score, respectively). These results constitute an initial baseline in an area where no prior results exist, as far as we know. Even if overall, the results need to be robustified to fully meet biologists’ expectations, the pipeline is complete and based on a promising state-of-the-art architecture. Therefore, we consider this study a handy baseline of an impactful extension to support new advances in Alzheimer’s disease. Moreover, building a fully operational pipeline will be crucial to create a 3D histology map for a deeper understanding of clinico-pathological associations in Alzheimer’s disease and the histology-based evidence of disease stratification among different sub-types.

**Keywords:** Alzheimer’s Disease, Tau Proteins, Tangles, Neuritic Plaques, Deep Learning, Computational Pathology, Whole Slide Images, Detection, Segmentation.

## 1. INTRODUCTION

Tau proteins are essential markers of Alzheimer’s Disease (AD) and probably present the best histopathological correlation with clinical symptoms.<sup>1</sup> However, it is yet unclear how these markers affect AD, qualitatively. Tau protein aggregates can be found in the gray matter within three types of structures: neurites, randomly and sparsely distributed proteins in neuronal processes; tangles, tau accumulations within the neuronal cell body; and neuritic plaques, spherical structures with tau positive dystrophic neurites surrounding Abeta positive core. We can find examples of these three different shapes in Figure 1.

In order to grasp their underlying behavior, we try to correlate the morphological variables associated with these protein aggregates and their spatial distribution in the brain with the advancement of the disease.

The state-of-the-art technology used to assess tau proteins is based on histological whole slide image (WSI) analysis. WSI consists of a slice of the (post-mortem) gray matter of an AD patient that is stained, observed with a microscope, and digitized with several magnification levels. Such WSI has a high magnification (x20, x40). A baseline for our work is the study presented by Signaevsky M., et al.,<sup>2</sup> where they focused on the neurofibrillary tangle segmentation in WSI. The authors reported an F1-score of 0.81 using a fully convolutional neural network (SegNet). In addition, Wurts, A., et al.,<sup>3</sup> study three deep learning models to segment neurofibrillary tangles

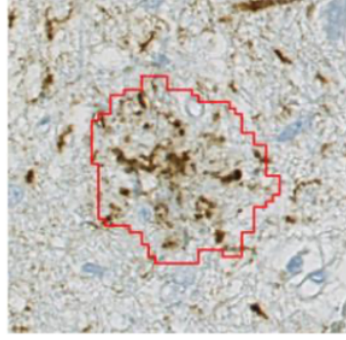
---

Further authors information: (Send correspondence to Daniel Racoceanu)

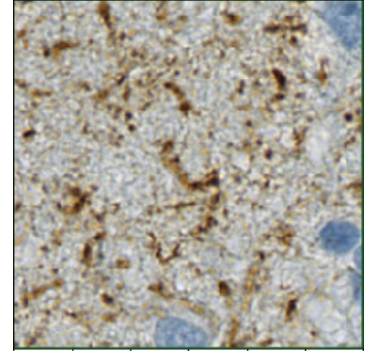
Daniel Racoceanu: E-mail: daniel.racoceanu@sorbonne-universite.fr, Telephone: +33 (0)6 33 77 42 67



(a) Example of *tangle* object (surrounded in red): the other brown stained little objects are *neurites*.



(b) *Plaque* object: brown stained little objects form the plaque neuritic crown surrounding the optically empty plaque core.



(c) Region only displaying tau-positive *neurites* (dark brown). Clearer objects form the background.

Figure 1: Examples of the 3 types of Tau proteins objects that can be found in the gray matter.

(NFT) and dystrophic neurites (DN). The authors combined color-based and manual annotations and reported an IoU of 0.611 using SegNet; however, they suggested the use of a pre-trained UNet to increase performance.

We present a novel end-to-end approach to process brain whole slide images based on convolutional neural network architectures and an Unet-based segmentation pipeline. In our study, the pipeline presented addresses not only the generation of an operational dataset suitable for a deep learning framework but also the models deployed to perform detection and segmentation of the different tau protein aggregates.

## 2. METHODOLOGY

### 2.1 Data preparation

#### a. *Raw data*

Raw data comprises six postmortem human whole slide images, labeled by pathologists with essentially four labels: background, tangles, neuritic plaques, and other (gray matter and neurites). The background being very fast to identify and annotate by a specialist, we focus on automatic separation between pixels on tangles, neuritic plaques, and gray matter/neurites. The differentiation between gray matter and neurites is also essential but easily performed using a simple stain classifier.

#### b. *Sampling*

To train and validate deep learning algorithms, we randomly sample fixed-size sub-images from WSI, controlling the fraction of images with tangles/neuritic plaques on them. The dataset so generated is called Balanced Random Sampling (BRS). We computed our results with a balance of 50/50 positive/negative sub-images. Once trained, we use the deep learning algorithm to retrieve and segment every tangle and neuritic plaque of a given WSI by exhaustively sampling it and feeding every sample to the model. We name it Exhaustive Deterministic Sampling (EDS) and use it as a test dataset.

#### c. *Stain normalisation*

Tau proteins' staining process is heterogeneous, hence a stain normalisation has been performed for the deep learning algorithm not having to cope with scaling issues. We tested various normalisation methods (i.e, histogram normalization, Macenko, Macenko-LS, Vahadane, Vahadane-LS, Reinhard, and Reinhard-LS) and ultimately, we retained 4 approaches. A different normalisation method was used for detecting and segmenting tangles and neuritic plaques. Additionally, we applied a pre-processing technique to datasets used for segmentation. It consists of standardising the brightness, i.e., modifying the luminosity channel so that 5% of pixels are fully luminous and thus white. We call this technique Standard Brightness (SB).

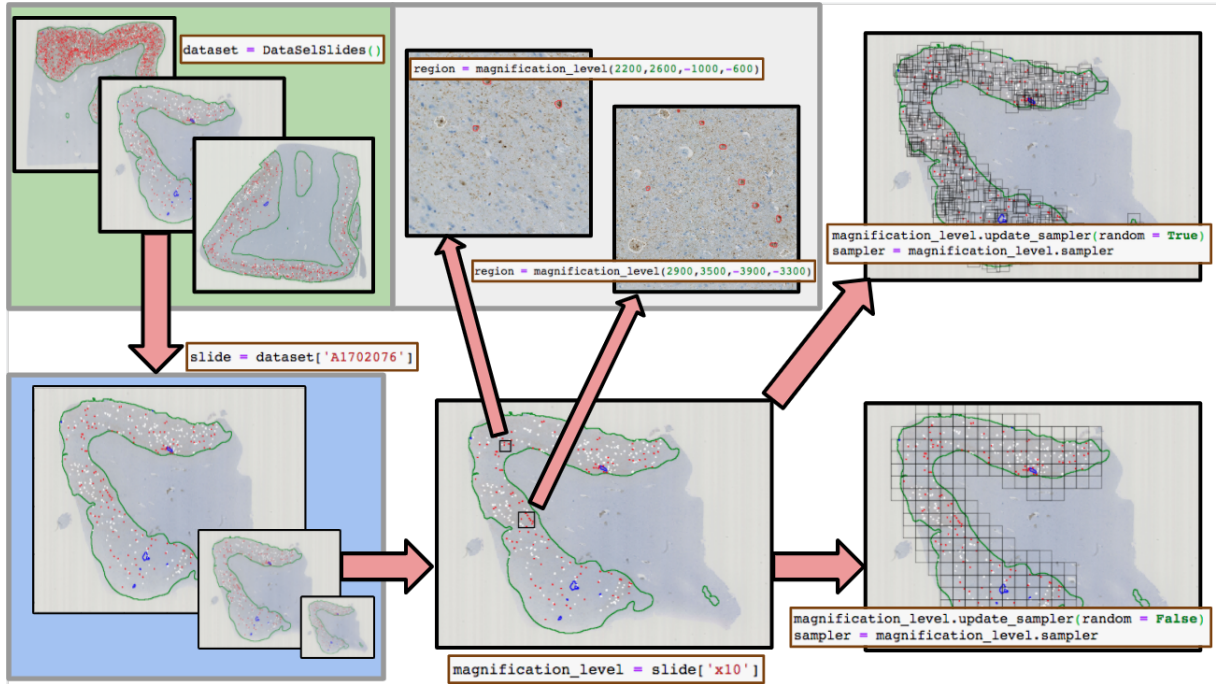


Figure 2: Whole pipeline for handling slides and their labels.

## 2.2 Deep learning pipeline architecture

### a. Tangles/neuritic plaques detection

Eliminating all samples showing no tangle nor neuritic plaques is crucial to further segmentation of these aggregates. Since this part aims to erase all samples with no tangles/neuritic plaques, one should raise precision while keeping recall extremely high. We used a convolutional-based deep learning architecture, 5 WSI for training and validation (80%/20% split), and 1 WSI for testing. We also implemented 5-fold cross-validation to assess the CNN generalisation to an independent dataset. Figure 3 represents this stage.

### b. Tangles/neuritic plaques segmentation

The segmentation algorithm is trained on 5 WSI using 5-fold cross-validation and tested on 1 WSI. The input test dataset, called Objects Only Sampling (OOS), provides only samples with tangles or neuritic plaque. We used an Unet-based architecture with a focal loss function. A quantitative study combined with an F1-score measure (computed assuming an intersection between a ground-truth segmentation and model segmentation to be a true positive) was used to evaluate the performances. Figure 4 represents this stage.

### c. Merging segmented regions

As a recap, during the test phase of segmentation, every region assessed by the classifier to be positive is segmented by the UNet model. We used this per-region segmentation to compute contour positions in meters corresponding to the slide at a global level. Furthermore, since some segmented objects may overlap or appear in two consecutive regions, we merged them by joining their corresponding contours. This stage allows for the reconstruction of the WSI and the computation of morphological features of the segmented objects.

## 3. RESULTS

In addition to the cross-validation process we implemented to evaluate the performance of the networks, we also applied a cross-testing scheme as shown in Table 1. Using this, we report the mean performance of the networks after having tested the models with different WSI. As it is shown in Table ??, the detection task performs effectively for tangle aggregates but needs improvements to achieve clinically operational results. The tangle segmentation task, however, provides state-of-the-art results never seen before, as far as we know. On the other

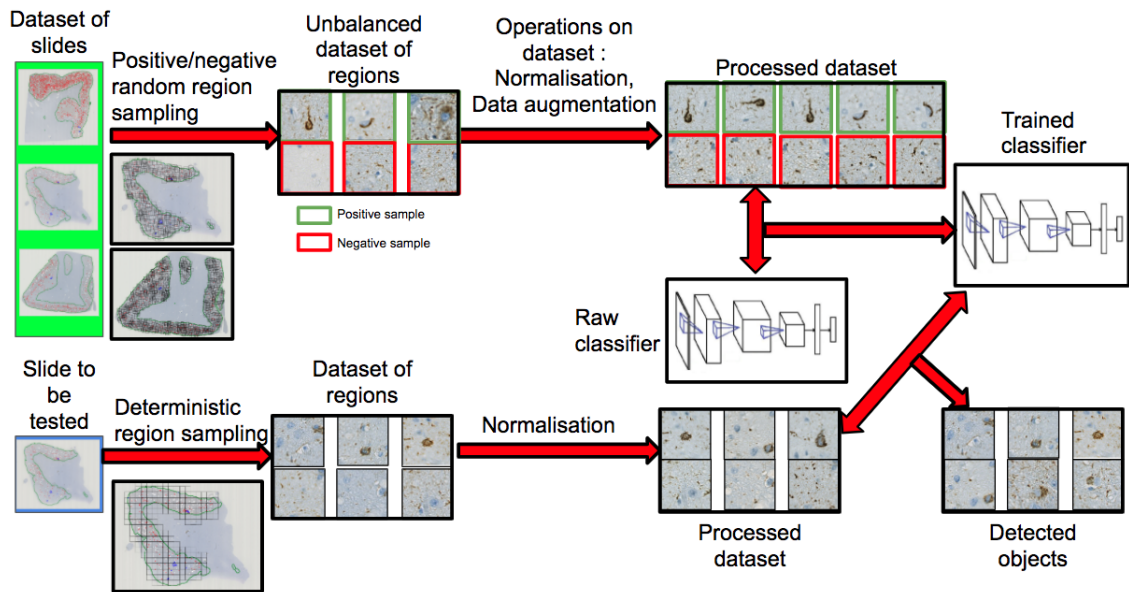


Figure 3: Overall scheme of detection of objects of interest on regions.

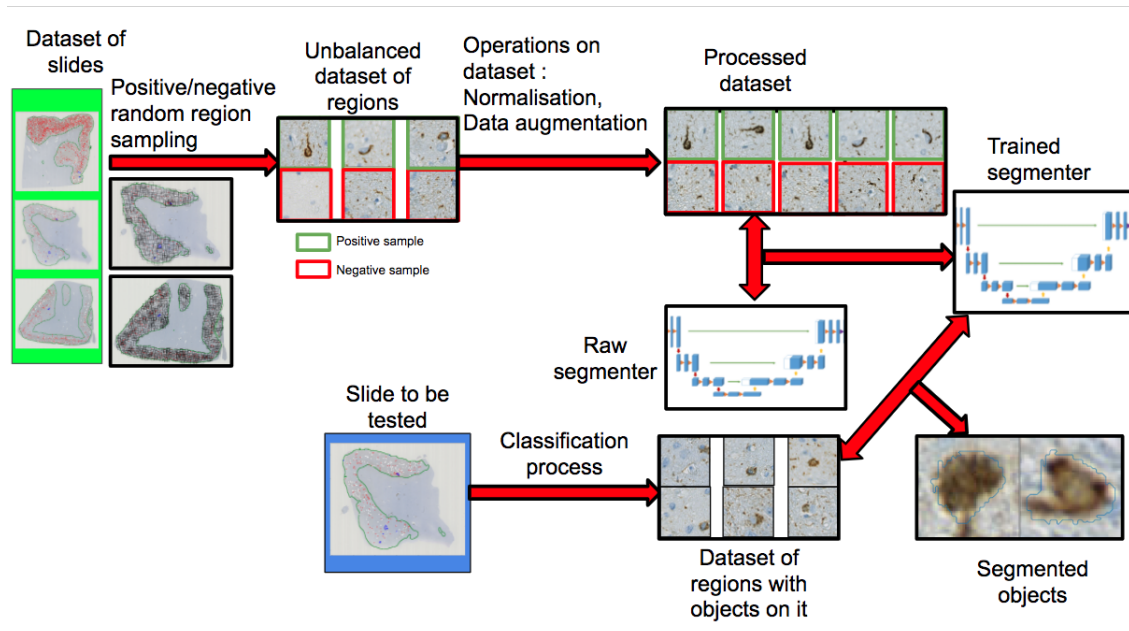


Figure 4: Overall scheme of segmentation of objects of interest on detected regions.

hand, the results shown represent an essential baseline for neuritic plaques detection and segmentation as no study has been reported with such results as far as we know. Neuritic plaques are very diffuse objects, and a pure segmentation may be hard to grasp for a model. Despite these difficulties (see Figure 6b), the segmentation results seem very encouraging.

#### 4. DISCUSSION AND CONCLUSION

This study has proven that we can generate clinically operational results by providing adequate WSI sampling and the proper normalization method. Future research will focus on bridging the gap between these promising

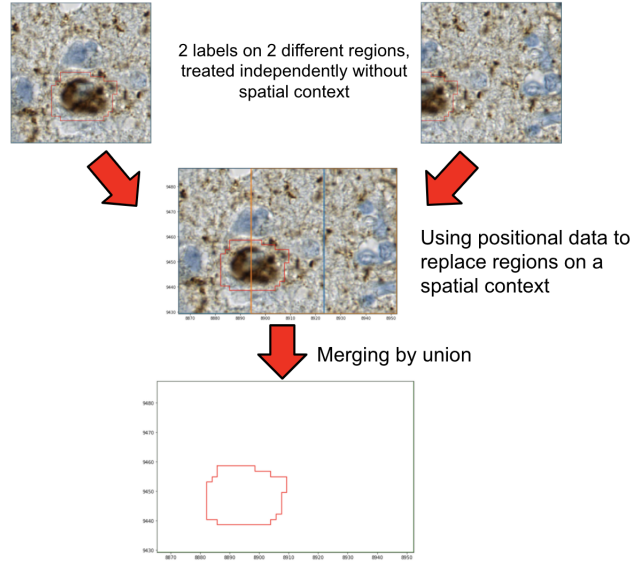


Figure 5: Illustration of merging of labels from different regions.

Table 1: Cross validation and cross testing procedure for segmentation and detection.

Train & validation					Test
WSI <sub>1</sub> ... WSI <sub>5</sub>					
FOLD 1	FOLD 2	FOLD 3	FOLD 4	FOLD 5	WSI <sub>6</sub>
FOLD 1	FOLD 2	FOLD 3	FOLD 4	FOLD 5	
FOLD 1	FOLD 2	FOLD 3	FOLD 4	FOLD 5	
FOLD 1	FOLD 2	FOLD 3	FOLD 4	FOLD 5	
FOLD 1	FOLD 2	FOLD 3	FOLD 4	FOLD 5	

...

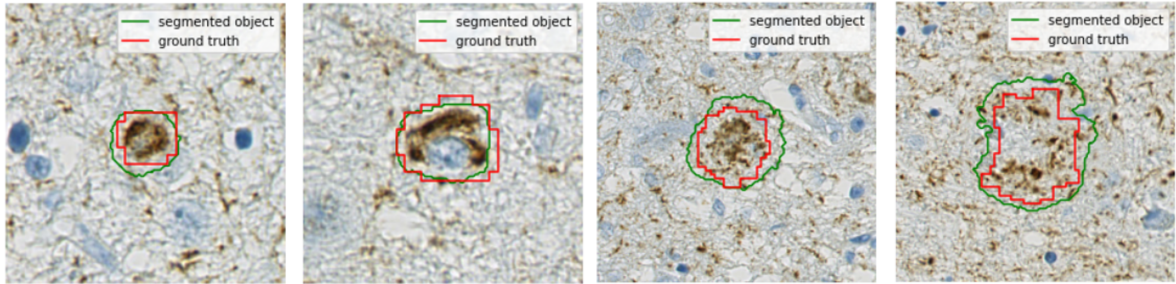
Train & validation					Test
WSI <sub>2</sub> ... WSI <sub>6</sub>					
FOLD 1	FOLD 2	FOLD 3	FOLD 4	FOLD 5	WSI <sub>1</sub>
FOLD 1	FOLD 2	FOLD 3	FOLD 4	FOLD 5	
FOLD 1	FOLD 2	FOLD 3	FOLD 4	FOLD 5	
FOLD 1	FOLD 2	FOLD 3	FOLD 4	FOLD 5	
FOLD 1	FOLD 2	FOLD 3	FOLD 4	FOLD 5	

Table 2: Results for detection of **tangles** and **plaques**.

Region	Train/validation			Test		
	Patch size (pixels)	Normalization	F1-score	Patch size (pixels)	Overlap (pixels)	F1-score
Neurofibrillary tangles	128 × 128	Histogram	99.6%	128 × 128	64	75.8%
Neuritic plaques	128 × 128	Macenko	99.8%	128 × 128	64	81.3%

Table 3: Results for segmentation of **tangles** and **plaques**.

Region	Train/validation			Test		
	Patch size (pixels)	Normalization	F1-score	Patch size (pixels)	Overlap (pixels)	F1-score
Neurofibrillary tangles	128 × 128	Reinhard (LS)	83.8%	128 × 128	64	91.1%
Neuritic plaques	128 × 128	Vahadane (LS)	81.5%	128 × 128	64	78.2%



(a) Examples of **tangle** segmentation.

(b) Examples of **neuritic plaques** segmentation.

Figure 6: Examples of the 3 types of tau proteins objects that can be found in the gray matter.

results and real use cases to reduce the number of false negatives samples driven by hyper-parameter tuning. In particular, an extension to this dataset with additional slides from different patients as well as different staining/scanning procedures might help robustify the pipelines presented in this work. Furthermore, from the segmented tau aggregates studied, a morphological analysis could also be implemented for Alzheimers' patients stratification and better understanding of this brain disorder.

Finally, the pipelines presented in this study could also be the core backend of an semi-supervised WSI annotator. This will definetly reduce the time pathologists spend in a single WSI and improve the annotations for the development of better AI tools.

## ACKNOWLEDGMENTS

This research is supported by Mr Jean-Paul Baudecroux and The Big Brain Theory Program - Paris Brain Institute (ICM).

## REFERENCES

- [1] Duyckaerts, C., Delatour, B., and Potier, M.-C., "Classification and basic pathology of Alzheimer disease," *Acta Neuropathologica* **118**, 5–36 (July 2009).
- [2] Signaevsky, M., Prastawa, M., Farrell, K., Tabish, N., Baldwin, E., Han, N., Iida, M. A., Koll, J., Bryce, C., Purohit, D., Haroutunian, V., McKee, A. C., Stein, T. D., White, C. L., Walker, J., Richardson, T. E., Hanson, R., Donovan, M. J., Cordon-Cardo, C., Zeineh, J., Fernandez, G., and Crary, J. F., "Artificial intelligence in neuropathology: deep learning-based assessment of tauopathy," *Laboratory Investigation* **99**, 1019–1029 (July 2019).
- [3] Wurts, A., Oakley, D. H., Hyman, B. T., and Samsi, S., "Segmentation of Tau Stained Alzheimers Brain Tissue Using Convolutional Neural Networks," in [*42nd Annual International Conference of the IEEE Engineering in Medicine & Biology Society (EMBC)*], 1420–1423, IEEE, Montreal, QC, Canada (July 2020).
- [4] Calderon-Garcidueñas, A. L. and Duyckaerts, C., "Chapter 23 - alzheimer disease," in [*Neuropathology*], Kovacs, G. G. and Alafuzoff, I., eds., *Handbook of Clinical Neurology* **145**, 325 – 337, Elsevier (2018).
- [5] Ronneberger, O., Fischer, P., and Brox, T., "U-net: Convolutional networks for biomedical image segmentation," *CoRR* **abs/1505.04597** (2015).
- [6] "Supplement 122: Specimen module and revised pathology sop classes," *Digital Imaging and Communications in Medicine (DICOM)* .
- [7] "Supplement 145: Whole slide microscopic image iod and sop classes," *Digital Imaging and Communications in Medicine (DICOM)* .
- [8] Bradski, G. and Kaehler, A., [*Learning OpenCV: Computer vision with the OpenCV library*], " O'Reilly Media, Inc." (2008).
- [9] Goode, A., Gilbert, B., Harkes, J., Jukic, D., and Satyanarayanan, M., "Openslide: A vendor-neutral software foundation for digital pathology," *Journal of pathology informatics* **4** (2013).
- [10] Gillies, S., "The shapely user manual," URL <https://pypi.org/project/Shapely> (2013).
- [11] Lin, T.-Y., Goyal, P., Girshick, R., He, K., and Dollár, P., "Focal loss for dense object detection," in [*Proceedings of the IEEE international conference on computer vision*], 2980–2988 (2017).
- [12] Kingma, D. P. and Ba, J., "Adam: A method for stochastic optimization," *arXiv preprint arXiv:1412.6980* (2014).
- [13] Tang, Z., Chuang, K. V., DeCarli, C., Jin, L.-W., Beckett, L., Keiser, M. J., and Dugger, B. N., "Interpretable classification of alzheimer's disease pathologies with a convolutional neural network pipeline," *Nature communications* **10**(1), 1–14 (2019).
- [14] Reinhard, E., Adhikhmin, M., Gooch, B., and Shirley, P., "Color transfer between images," *IEEE Computer graphics and applications* **21**(5), 34–41 (2001).
- [15] Macenko, M., Niethammer, M., Marron, J. S., Borland, D., Woosley, J. T., Guan, X., Schmitt, C., and Thomas, N. E., "A method for normalizing histology slides for quantitative analysis," in [*2009 IEEE International Symposium on Biomedical Imaging: From Nano to Macro*], 1107–1110, IEEE (2009).

- [16] Khan, A. M. et al., “A nonlinear mapping to stain normalization in digital histopathology images using image-specific color deconvolution,” *IEEE TBME* **61**(6), 1729–1738 (2014).
- [17] Janowczyk, A. and Madabhushi, A., “Deep learning for digital pathology image analysis: A comprehensive tutorial with selected use cases,” *Journal of pathology informatics* **7** (2016).
- [18] Song, J., Xiao, L., Molaei, M., and Lian, Z., “Multi-layer boosting sparse convolutional model for generalized nuclear segmentation from histopathology images,” *Knowledge-Based Systems* **176**, 40–53 (2019).
- [19] Zemouri, R., Zerhouni, N., and Racoceanu, D., “Deep learning in the biomedical applications: Recent and future status,” *Applied Sciences* **9**(8), 1526 (2019).
- [20] Huang, G., Liu, Z., Van Der Maaten, L., and Weinberger, K. Q., “Densely connected convolutional networks,” in [*Proceedings of the IEEE conference on computer vision and pattern recognition*], 4700–4708 (2017).
- [21] Simonyan, K. and Zisserman, A., “Very deep convolutional networks for large-scale image recognition,” *arXiv preprint arXiv:1409.1556* (2014).
- [22] He, K., Zhang, X., Ren, S., and Sun, J., “Deep residual learning for image recognition,” in [*Proceedings of the IEEE conference on computer vision and pattern recognition*], 770–778 (2016).
- [23] Litjens, G., Kooi, T., Bejnordi, B. E., Setio, A. A. A., Ciompi, F., Ghafoorian, M., Van Der Laak, J. A., Van Ginneken, B., and Sánchez, C. I., “A survey on deep learning in medical image analysis,” *Medical image analysis* **42**, 60–88 (2017).
- [24] Bankhead, P., Loughrey, M. B., Fernández, J. A., Dombrowski, Y., McArt, D. G., Dunne, P. D., McQuaid, S., Gray, R. T., Murray, L. J., Coleman, H. G., et al., “Qupath: Open source software for digital pathology image analysis,” *Scientific reports* **7**(1), 1–7 (2017).
- [25] Vahadane, A., Peng, T., Albarqouni, S., Baust, M., Steiger, K., Schlitter, A., Sethi, A., Esposito, I., and Navab, N., “Structure-preserved color normalization for histological images,” 1012–1015 (04 2015).